BENTHIC FORAMINIFERAL OXYGEN ISOTOPE OFFSETS OVER THE LAST GLACIAL-INTERGLACIAL CYCLE

Babette Hoogakker, Harry Elderfield, Kevin Oliver, Simon Crowhurst

Abstract

The oxygen isotope ($\delta^{18}O$) offset between contemporaneous benthic foraminiferal species is often assumed constant with time and geographic location. We present an inventory of benthic foraminiferal species $\delta^{18}O$ offsets from the major ocean basins covering the last glacial-interglacial cycle, showing that of the twenty down-core records investigated, twelve show significant temporal changes in $\delta^{18}O$ offsets that do not resemble stochastic variability. Some of the temporal changes may be related to kinetic fractionation effects causing deglacial/interglacial enrichment or glacial depletion in mainly infaunal species, but additional research is needed to confirm this. In addition to stratigraphic implications the finding of temporally varying offsets between co-existing benthic foraminiferal species could have implications for sea-level, deep water temperature, and regional deep water $\delta^{18}O$ estimates.

1. Introduction

Because of the varying occurrence and abundance of individual benthic foraminiferal species in relation to changing environmental conditions, many paleoceanographic studies are not able to use a single benthic foraminifera species to create continuous oxygen isotope ($\delta^{18}O$) records. In order to generate continuous records, composite records are generated, taking into account isotope offsets between different co-existing species. An important assumption, often made, is that such offsets are constant with time and geographical location.

At the same oceanic location co-existing benthic foraminiferal species often have different $\delta^{18}O$, making it unlikely that all species form their calcite in equilibrium with seawater (Duplessy et al., 1970). For example, some authors have suggested that the $\delta^{18}O$ of *Uvigerina peregrina* reflects $\delta^{18}O$ equilibrium (Shackleton, 1974; Woodruff et al., 1980; McCorkle et al., 1990), whereas use of a more recent inorganic $CaCO_3$ temperature - $\delta^{18}O$ fractionation curve (Kim and O'Neil, 1997) suggests that *Cibicidoides* $\delta^{18}O$ is in equilibrium with sea-water whereas *Uvigerina* $\delta^{18}O$ is not (Bemis et al., 1998).

Additional secondary factors that influence benthic foraminiferal $\delta^{18}O$ include: 1- kinetic fractionation effects during hydration and hydroxylation of CO_2 related to carbonate chemistry (Spero et al., 1997; Bijma et al., 1999; Zeebe, 1999), 2- metabolic fractionation effects during biomineralization related to species specific vital effects (Duplessy et al., 1970; Shackleton, 1974; Schmiedl and Mackensen, 2006), and 3- preservation effects related to dissolution and respiration (Broecker and Peng, 1982, Mackensen et al., 1993; Schmiedl and Mackensen, 2006).

Important assumptions in many paleoceanographic studies are that the $\delta^{18}O$ offset between inorganic calcite precipitated in equilibrium (e.g. see Kim and O'Neil, 1997) and benthic foraminiferal calcite is constant, and that the offset between the $\delta^{18}O$ of co-existing benthic foraminiferal species is constant. Here we monitor benthic foraminiferal $\delta^{18}O$ offsets between commonly used benthic foraminiferal species by comparing the isotope data obtained from co-existing species over the last glacial-interglacial cycle. Additionally we compare down-core $\delta^{18}O$ offset records with co-existing $\delta^{13}C$ records to explore whether down-core $\delta^{18}O$ offset variations may be related to kinetic fractionation effects through changes in organic matter fluxes/decomposition (Fontanier et al., 2006; Schmiedl and Mackensen, 2006).

2. Material & method

This study forms part of a data synthesis effort to improve links between proxy data and mechanistic understanding through Earth system models (http://researchpages.net/QQ), and is largely based on isotope data obtained from data repositories (PANGAEA, NCDC, DELPHI) measured by various laboratories. By using isotope data measured by different laboratories we cannot entirely exclude inter-laboratory offsets such as from cleaning, sample size, standards and equipment used etc. However, for most of the down-core records stable isotope analysis on co-existing benthic foraminiferal species were performed at the same laboratory, thus allowing species-species comparison.

Down-core benthic foraminiferal $\delta^{18}O$ (and $\delta^{13}C$) data were assembled for records containing multiple species $\delta^{18}O$ (a total of 39 records) for the last 150,000 years containing data for thirteen species (*Cibicidoides/Planulina/Fontbotia wuellerstorfi*, here referred to as *C. wuellerstorfi*, *Cibicidoides kullenbergi*, *Cibicidoides pachyderma*, *Cibicides lobatulus*, *Planulina ariminensis*, *Oridorsalis umbonatus, Oridorsalis tener, Uvigerina excellens, Uvigerina hollicki, Uvigerina mediterranea, Uvigerina peregrina, Melonis barleeanum, Globobulimina affinis*). Core locations are shown in Figure 1, and details of latitude, longitude, water depth, and benthic foraminiferal species are listed in online supporting material (Table S1). Currently available information on habitat requirements of specific benthic foraminiferal species is summarized in on-line supporting material (Table S2).

3. Results

Histograms of benthic foraminiferal $\delta^{18}O$ offsets (epifaunal minus infaunal and infaunal minus deeper infaunal) were plotted for five benthic foraminiferal pairs (*C. wuellerstorfi* vs. *U. peregrina*, *U. hollicki*, *M. barleeanum*, *G. affinis* and *U. peregrina* vs. *G. affinis*) combining between 2 and 14 down-core records with a total of at least 100 data points (Figure 2A). Offsets of the remaining benthic foraminiferal sets can be found in online supporting material (Figure S1). A summary of mean benthic foraminiferal $\delta^{18}O$ offsets for all benthic foraminiferal pairs is provided in Table 1. The calculated average benthic foraminiferal $\delta^{18}O$ offsets agree well with those reported in the literature (e.g. Shackleton et al., 2000; Schmiedl and Mackensen,

2006) (Figure 2A, Table 1). Mean benthic foraminiferal $\delta^{18}O$ offsets are generally lowest (close to 0‰) for epifaunal species pairs (for example *C. lobatulus* vs. *C. pachyderma* and *C. wuellerstorfi* vs. *C. kullenbergi*; however, we note the different $\delta^{18}O$ offset between *C. wuellerstorfi* vs. *P. ariminensis* (0.43‰)), and highest between epifaunal and deep infaunal species (e.g. *C. wuellerstorfi* vs. *G. affinis* (-0.90‰)) (Table 1, Figure 2A). Offsets between epifaunal *C. wuellerstorfi* and infaunal *M. barleeanum*, for which the majority (85%) of samples are from Arabian Sea core GeoB-3004-1, are relatively low with a mean of -0.18‰ (Table 1).

Scatter-plots of the five benthic foraminiferal sets (the remaining sets can be found in online supporting material Figure S1) show significant correlations between *C. wuellerstorfi* vs. *G. affinis*, *U. hollicki*, *U. peregrina* and *M. barleeanum* $\delta^{18}O$, which is confirmed by student-t distribution tests (Figure 2B; online supporting material Table S3). However, for *C. lobatulus* vs. *C. pachyderma*, *C. wuellerstorfi* vs. *P. ariminensis*, *C. wuellerstorfi* vs. *U. excellens*, and *U. peregrina* vs. *M. barleeanum* $\delta^{18}O$ correlations are weak ($R < 0.6$), whereas *C. wuellerstorfi* vs. *O. tener* and *U. mediterranea* $\delta^{18}O$ are not significantly correlated (online supplementary material Figure S1, Table S3). The isotopic ranges of closely correlated benthic foraminiferal species $\delta^{18}O$ are similar, except for *C. wuellerstorfi* (2.1‰) vs. *G. affinis* (2.6‰) (Figure 2B).

Of all the cores investigated, twenty (indicated in Figure 1 with open circles) contained sufficient data (>15 sample pairs) and well constrained age models for the last <150,000 years to compare interspecific $\delta^{18}O$ offsets for specific stratigraphic time windows. In Figure 3, six examples are shown of records with epifaunal and infaunal benthic foraminiferal $\delta^{18}O$ (*C. wuellerstorfi* vs. *U. peregrina* and *U. hollicki*) and their offsets. Plots of all other down-core records can be found in online supplementary material Figure S2. Offsets are plotted against depth (m) down-core and significant climatic intervals are marked (Figure 3). Where available, AMS ^{14}C ages are plotted. We split the benthic foraminiferal $\delta^{18}O$ offset records into records that show no temporal variations (A) and records that show small (0.2 to 0.5‰) to large (>0.5‰) temporal variations of $\delta^{18}O$ offsets (B, C, Figure 3). Only cores where differences in offset exceed that of the standard deviation of the offset were classified as having temporal variations. Of the twenty cores, twelve were classified as having temporal variations in benthic foraminiferal $\delta^{18}O$ offsets. Of the benthic foraminiferal

$\delta^{18}O$ pairs (for several cores isotope data was available for more than two benthic foraminiferal species) a total of sixteen to seventeen out of twenty nine pairs showed temporal variations in their offsets (Figure 3, online supplementary material Figure S2).

In Figure 4 we compare the benthic epifaunal-infaunal foraminiferal $\delta^{18}O$ offset records of Figure 3 with co-existing benthic foraminiferal $\delta^{13}C$ and $\delta^{13}C$ offset records (remaining records are shown in online supplementary material Figure S3).

4. Discussion

4.1 Causes for temporal changes in benthic foraminiferal $\delta^{18}O$ offsets

Differential bioturbation effects have been used to explain variations in benthic foraminiferal $\delta^{18}O$ offsets, especially at low sedimentation rate locations (Zahn et al., 1986). However the intervals showing different benthic foraminiferal $\delta^{18}O$ offsets in this work are between 0.2 and 1.3 m deep and generally exceed the typical length scales for bioturbation (Figure 3, supplementary material Figure S2) suggesting other causes may be responsible for the changes in benthic foraminiferal $\delta^{18}O$ offsets. These include a change in dominant morphotype, although for morphotypes of *C. wuellerstorfi* from the east Timor Sea there appears to be no difference in $\delta^{18}O$ and $\delta^{13}C$ (Dürkop et al., 2008).

To test whether environmental settings are key to down-core co-existing benthic foraminiferal $\delta^{18}O$ offsets, we focus our discussion on records that involve comparisons between *C. wuellerstorfi* vs. *U. peregrina* and *U. hollicki* as these make up the majority of records (thirteen out of twenty records, with nine showing temporal variations) and involve more commonly used benthic foraminiferal species in paleoceanographic reconstruction. Comparison is made between records from the low oxygen Arabian Sea, open Atlantic and the highly-productive West African Margin (Figure 5).

The average $\delta^{18}O$ offsets between *C. wuellerstorfi* and the two *Uvigerina* species are identical (Table 1). Temporal offset variations between *C. wuellerstorfi* vs. *U. peregrina* and *U. hollicki* are the result of either: deglacial/interglacial enrichment in *Uvigerina* (six records), or glacial depletion in *Uvigerina* (three records) (Figure 3, online supplementary material Figure S2). Glacially depleted *Uvigerina* $\delta^{18}O$ is only observed along the highly productive West African Margin, whereas

deglacial/interglacial enrichments also occur in the low oxygen Arabian Sea and open Atlantic Ocean (Figure 5). Clearly the deglacial/interglacial enrichment and glacial depletion in *Uvigerina* are due to secondary effects, including dissolution effects, metabolic fractionation, and/or kinetic fractionation.

Dissolution effects seem unlikely; at Arabian Sea core GeoB3004-1, where the largest temporal offset variations occur between *C. wuellerstorfi* and *U. peregrina*, Schmiedl and Mackensen (2006) did not observe dissolution effects on recent *U. peregrina*, and there is no straightforward relation between *C. wuellerstorfi* - *U. peregrina* $\delta^{18}O$ offset and calcite dissolution (see online supporting material Figure S4). Changes in metabolic activity may affect isotope fractionation. Metabolic activity may be more intense in juveniles (Berger et al., 1978), or be increased under higher temperatures (Moberly, 1968), but the effects are unpredictable (Zhou and Zheng, 2003). Most down-core dual benthic foraminiferal $\delta^{18}O$ records are based on measurements of large adult specimens (see online supplementary information Table S1), and although warmer deep- and intermediate water temperatures (Waelbroeck et al., 2002) during deglaciations/interglacials may have increased (infaunal) benthic foraminiferal metabolic activity, the non-coherent distribution of records characterized and uncharacterized by temporal offset changes (Figure 5) does not support a metabolic effect.

Planktonic foraminiferal culture experiments show that decreasing (increasing) carbonate ion (CO_3^{2-}) concentrations cause an increase (decrease) in calcite $\delta^{18}O$ and $\delta^{13}C$ (Spero et al., 1997). A similar effect has been proposed to influence benthic foraminifera $\delta^{18}O$ and $\delta^{13}C$ (Mackensen and Licari, 2004; Schmiedl et al., 2004), but this would require a much greater sensitivity to CO_3^{2-} than for planktonic foraminifera. For the records where the *C. wuellerstorfi* - *Uvigerina* $\delta^{18}O$ offsets variations are caused by interglacial enrichment in *Uvigerina* (by 0.4 to 0.8‰) (Table 1), use of the CO_3^{2-} - $\delta^{18}O$ relationship of Spero et al (1997) would result in large, and unrealistic, localized decreased deglacial/interglacial CO_3^{2-} of 200 to 400 μmol/kg. For the records where the offset variations are caused by glacial depletion in *Uvigerina* (-0.3 to 1.2‰) unrealistic high glacial CO_3^{2-} (increased by 150 to 600 μmol/kg) would be needed. A greater (×4.5) sensitivity of benthic foraminiferal $\delta^{18}O$ to CO_3^{2-} is confirmed by a recent study of Rathmann and Kuhnert (2008), based on recent *O. umbonatus* from core tops from the Namibian continental slope, and would

result in more realistic porewater CO_3^{2-} changes of -111 to -67 μmol/kg from the last glacial to interglacial to cause deglacial/interglacial enrichment in *Uvigerina* $\delta^{18}O$, and +56 to +155 μmol/kg to cause glacial depleted $\delta^{18}O$ in *Uvigerina*. In the planktonic foraminiferal culture experiments calcite $\delta^{13}C$ also increases with decreasing CO_3^{2-} (Spero et al., 1997), and so a similar effect may be expected in benthic foraminiferal $\delta^{13}C$. Only two records (GIK13292-1, VIK13519-1) characterized by $\delta^{18}O$ offset variations caused by deglacial/interglacial enrichment in *U. peregrina* show contemporary interglacial $\delta^{13}C$ enrichments (up to 0.8‰) compared with *C. wuellerstorfi*, whereas the remaining records show $\delta^{13}C$ depletion or no effect (Figure 4, online supplementary material Figure S4). In the low oxygen Arabian Sea $\delta^{18}O$ offset variations resulting from deglacial/interglacial ^{18}O enriched *U. peregrina*, have been linked to increased remineralization of organic material during interglacials (Schmiedl and Mackensen, 2006; Gupta et al., 2008). One possibility for an absence of deglacial $\delta^{13}C$ enrichment in *Uvigerina* $\delta^{13}C$ and perhaps even depletion at higher productivity locations could be related to high remineralization rates of organic material causing increased release of light ^{12}C and decrease in benthic foraminiferal $\delta^{13}C$, thus counteracting the $\delta^{13}C$ increase caused by the inferred CO_3^{2-} decrease.

For the other records from the West African Margin where the offset variations are caused by glacially depleted *Uvigerina* $\delta^{18}O$ (e.g. GIK 16030-1, GIK 12328-5 and GIK 12309-1), increased glacial CO_3^{2-} concentrations would be needed. Glacial Atlantic intermediate water CO_3^{2-} may have been increased, but the deeper sites (GIK12328-5 and GIK12309-1) were likely bathed in low CO_3^{2-} Glacial Antarctic Bottom Waters (Curry and Oppo, 2005; Sarnthein et al., 1994; Yu et al., 2008). In the present day north east Arabian Sea *U. peregrina* specimens living inside bacterial mats within the oxygen minimum zone have depleted $\delta^{18}O$ values compared with specimens living outside the mat (Erbacher and Nelskamp, 2006). Perhaps similar environmental conditions are responsible for depleted glacial *U. peregrina* $\delta^{18}O$ off West Africa. In both cases (bacterial mats, glacial West African Margin), depleted *Uvigerina* $\delta^{18}O$ was not accompanied by depleted $\delta^{13}C$ (in fact no effect was observed in the West African Margin records, even though productivity and export were enhanced during the last glacial (Abrantes, 2000; Kohfeld et al., 2005)), providing support that similar mechanism may be responsible for the depletions in

$\delta^{18}O$. In-depth multi-proxy research (down-core and culturing) is needed to asses the potential role of seawater CO_3^{2-}, metabolic and other effects on (infaunal) benthic foraminiferal $\delta^{18}O$.

4.2 Implications

This review reveals relatively large variability in benthic foraminiferal $\delta^{18}O$ offsets (standard deviations between 0.22 to 0.66‰, which is significantly larger than analytical (external i.e., including sample gas generation plus instrumental precision) reproducibility of isotope analysis that typically is better than ~0.08‰). This may affect the interpretation of composite records based on multiple benthic foraminiferal species, and comparison of records from different locations that were measured using different monospecific benthic foraminiferal species or composite records, where a constant adjustment is made.

Relatively large uncertainties may therefore be added to studies using composite benthic foraminiferal $\delta^{18}O$ records to infer sea-level changes, and deepwater temperatures. Taking a standard deviation of 0.2‰ of the $\delta^{18}O$ offset between benthic foraminiferal species into account potentially contributes 25 m uncertainty to sea-level reconstructions and a ~1ºC uncertainty to deepwater temperature reconstructions). Exclusion of suspect deglacial/interglacial and glacial outliers improves the linear correlation between $\delta^{18}O$ pairs of *C. wuellerstorfi* vs. *U. peregrina* and *U. peregrina* vs. *G. affinis* and reduces their mean $\delta^{18}O$ offset standard deviations (Figure 6). Standard deviations of $\delta^{18}O$ offsets between species along a single sediment core are lower on occasion although the majority fall close to 0.2‰ (Table 1). In order to minimize uncertainties it is recommended to use locally derived benthic foraminiferal offsets for the construction of multi-species benthic foraminiferal $\delta^{18}O$ records.

The majority of down-core records examined display temporal variations in benthic foraminiferal $\delta^{18}O$ offsets (Figure 5). These occur for paired epifaunal-epifaunal, epifaunal-infaunal, and infaunal-infaunal benthic foraminiferal $\delta^{18}O$ at a wide range (800-4000 m) of water depths (Table 1, Figure 5). All down-core benthic foraminiferal $\delta^{18}O$ offset records are from the Atlantic (19 records) and Indian Ocean (1 record) (Figure 5); isotope records from the Pacific contained only a small number of (>15) $\delta^{18}O$ pairs for the last 150,000 years that was insufficient to robustly assess $\delta^{18}O$ variability through time between different benthic species.

The finding of temporal changes in inter-species $\delta^{18}O$ offsets has potential stratigraphic implications. Not knowing $\delta^{18}O$ enrichments within parts of monospecific *U. peregrina* $\delta^{18}O$ records may add uncertainty to the identification of Marine Isotope Stage boundaries and hinder the core-to-core correlation of finer-scale (sub-Milankovich) variability along benthic $\delta^{18}O$ records. Variations through time of interspecific benthic $\delta^{18}O$ also bear implications for sea-level, deep water temperature, and local deep water $\delta^{18}O$ reconstructions. Variable $\delta^{18}O$ enrichment in benthic foraminiferal tests due to changing seawater carbonate chemistry (CO_3^{2-}) constitutes a further uncertainty that potentially affects the paleo-hydrographic interpretation of benthic $\delta^{18}O$ records. Hence benthic foraminiferal $\delta^{18}O$ offset variations and variable $\delta^{18}O$ enrichment in individual benthic species needs to be considered when interpreting monospecific infaunal and in particular, composite multiple-species benthic foraminiferal $\delta^{18}O$ records.

5. Conclusions

The hypothesis that benthic foraminiferal $\delta^{18}O$ offsets of widely used benthic foraminiferal species are constant is tested using existing isotope data covering the last glacial-interglacial cycle.

Of the twenty down-core $\delta^{18}O$ offset records investigated, thirteen showed significant temporal offset variations (exceeding the offset standard deviation) that are not related to short-term random variability. These temporal changes in benthic foraminiferal offsets may be related to kinetic fractionation effects, with changes in porewater CO_3^{2-}, leading to $\delta^{18}O$ enrichment and depletion in infaunal species, but this mechanism needs to be confirmed by further research. Temporal $\delta^{18}O$ enrichment and depletion in mainly infaunal species can have implications for stratigraphy and estimates of sea-level, deep water temperature and local deep water $\delta^{18}O$ studies.

Acknowledgements

This research was funded by Quaternary Quest (NERC). Careful and critical reviews by F. Jorissen, two anonymous reviewers and the editor (R. Zahn) significantly improved the contents of this manuscript.

References

Abrantes, F., 2000. 200,000 yr diatom records from Atlantic upwelling sites reveal maximum productivity during LGM and shift in phytoplankton community structure at 185,000 yr. Earth and Planetary Science Letters 176, 7-16.

Bauch, H.A, Erlenkeuser, H., Spielhagen, R.F., Struck, U., Matthiessen, J., Thiede, J., Heinemeier, J., 2001. A multiproxy reconstruction of the evolution of deep and surface waters in the subarctic Nordic seas over the last 30,000 years. Quaternary Science Reviews 20, 659-678.

Bemis, B.E., Spero, H.J., Bijma, J., Lea, D.W., 1998. Re-evaluation of the oxygen isotopic composition of planktonic foraminifera: Experimental results and revised temperature equations. Paleoceanography 13, 150-160.

Berger, W.H., Killingley, J.S., Vincent, E., 1978. Stable isotopes in deep sea carbonates: Box core ERDC 92 west equatorial Pacific. Oceanologica Acta 1, 203-216.

Berger, W.H., Killingley, J.S., Metzler, C.V., Vincent, E., 1985. Two-Step Deglaciation: 14C-Dated High Resolution $\delta^{18}O$ Records from the Tropical Atlantic Ocean. Quaternary Research 23, 258-271.

Bijma, J., Spero, H.J., Lea, D.W., 1999. Reassessing foraminiferal stable isotope geochemistry: impact of the ocean carbonate system (experimental results). From Fischer, G., Wefer, G. (Eds) Use of proxies in paleoceanography: examples from the South Atlantic. Springer-Verlag Berlin Heidelberg, pp. 489-512.

Broecker, W.S., Peng, T.H., 1982. Tracers in the Sea, Lamont–Doherty Geological Observations, Columbia University, New York, 690 pp.

Bühring, C., 2001. East Asian Monsoon variability on orbital- and millennial-to-sub-decadal time scales. PhD Thesis, Mathematisch-Naturwissenschaftliche Fakultät der Christian-Albrechts-Universität zu Kiel, 164 pp.

CLIMAP Project Members 1981. Seasonal reconstruction of the earth's surface at the last glacial maximum, Geological Society of America, Map and Chart Series, 36.

Curry, W.B., Duplessy, J.C., Labeyrie, L.D., Shackleton, N.J., 1988. Changes in the distribution of δ13C of deep water ΣCO2 between the last glaciation and the Holocene, Paleoceanography, 3, 317–341.

Curry, W.B., Oppo, D.W., 2005. Glacial water mass geometry and the distribution of $\delta^{13}C$ of ΣCO_2 in the western Atlantic Ocean. Paleoceanography 20, PA1017, doi:10.1029/2004PA001021.

Duplessy, J.C., Lalou, C., Vinot, A.C., 1970. Differential isotopic fractionation in benthic foraminifera and paleotemperatures assessed. Science 168, 250-251.

Duplessy, J.C., Labeyrie, L., Blanc, P.L., 1988. Norwegian Sea Deep Water variations over the last climatic cycle: Paleo-oceanographical implications. In Wanner, H. & Siegenthaler, U. (eds.), Long and short term variability of climate, Springer (Heidelberg), 83-116.

Duplessy, J.-C. 1996. Quaternary paleoceanography: unpublished stable isotope records. IGBP PAGES/World Data Center for Paleoclimatology Data Contribution Series 1996-035. NOAA/NGDC Paleoclimatology Program, Boulder, Colorado, USA.

Dürkop, A., Holbourn, A., Kuhnt, W., Zuraida, R., Andersen, N., Grootes, P.M., 2008. Centennial-scale climate variability in the Timor Sea during Marine Isotope Stage 3. Marine Micropaleontology 66, 208-221.

Erbacher, J., Nelskamp, S., 2006. Comparison of benthic foraminifera inside and outside a sulphur-oxidizing bacterial mat from the present oxygen-minimum zone off Pakistan (NE Arabian Sea). Deep-Sea Research I 53, 751-775.

Fontanier, C., Mackensen, A., Jorissen, F.J., Anschultz, P., Licari, L., Griveaud, C., 2006. Stable oxygen and carbon isotopes of live benthic foraminifera from the Bay of Biscay: Microhabitat impact and seasonal variability. Marine Micropaleontology 58, 159-183.

Gupta, A.K., Das, M., Clemens, S.C., Mukherjee, B., 2008. Benthic foraminiferal faunal and isotopic changes as recorded in Holocene sediments in the northwest Indian Ocean. Paleoceanography 23, doi:10.1029/2007PA001546.

Hagen, S., Keigwin, L.D., 2002. Sea-surface temperature variability and deep water reorganisation in the subtropical North Atlantic during Isotope Stage 2-4. Marine Geology 189, 145-162.

Hodell, D.A., Charles, C.D., Curtis, J.H., Mortyn, P.G., Ninnemann, U.S., Venz, K.. 2003. Data Report: calcareous nannofossil data from the Eocene to Oligocene, Leg 177, Hole 1090B. In: Gersonde, R., Hodell, D.A., and Blum, P. (eds.), Proc. ODP, Sci. Results. Available from World Wide Web, 177, 1-26.

Kim, S.T., O'Neil, J.R., 1997. Equilibrium and non-equilibrium oxygen isotope effects in synthetic calcites. Geochimica et Cosmochimica acta 33, 1-17.

Kohfeld, K.E., Le Quéré, C., Harrison, S.P., Anderson, R.F., 2005. Role of marine biology in glacial-interglacial CO_2 cycles. Science 308, 74-78.

Labeyrie, L., Duplessy, JC., 1985. Changes in the oceanic 13C/12C ratio during the last 140,000 years: high latitude surface water records. Palaeogeography, Palaeoclimatology, Palaeoecology 50, 217-240.

Labeyrie, L., Vidal, L., Cortijo, E., Paterne, M., Arnold, M., Duplessy, J.C., Vautravers, M., Labracherie, M., Duprat, J., Turon, J.L., Grousset, F., Van Weering, T., 1995. Surface and deep hydrology of the Northern Atlantic Ocean during the last 150,000 years. Philosophical Transactions of the Royal Society of London, B 348:255-264.

Labeyrie, L., Labracherie, M., Gorfti, N., Pichon, J.J., Vautravers, M.J., Arnold, M., Duplessy, J.C., Paterne, M., Michel, E., Duprat, J., Caralp, M., Turon, J.L., 1996. Hydrographic changes of the Southern Ocean (southeast Indian sector) over the last 230 kyr. Paleoceanography 11, 57-76.

Mackensen, A., Licari., L. 2004. Carbon sotopes of live benthic foraminifera from the South Atlantic: Sensitivity to bottom water carbonate saturation state and organic matter rain rates, in The South Atlantic in the Late Quaternary: Reconstruction of Material Budget and Current Systems, edited by G. Wefer, S. Mulitza, and V. Rathmeyer, pp. 623– 644.

Mackensen, A., Hubberten, H.W., Bickert, T., Fischer, G., Futterer, D.K., 1993. The delta-C-13 in benthic foraminiferal tests of Fontbotia wuellerstorfi (Schwager) relative to delta-C-13 of dissolved inorganic carbon in Southern Ocean Deep Water - implications for glacial ocean circulation models. Paleoceanography 8, 587-610.

McCorkle, D.C., Keigwin, L.D., Corliss, B.H., Emerson, S.R., 1990. The influence of microhabitats on the carbon isotopic composition of deep-sea benthic foraminifera, Paleoceanography, 5, 161– 185.

Moberly, R., 1968. Composition of magnesium calcites algae and pelecypods by electron microprobe analysis. Sedimentology 11, 61-82.

Rathmann, S., Kuhnert, H., 2007. Carbonate ion effect on Mg/Ca, Sr/Ca and stable isotopes on the benthic foraminifera *Oridorsalis umbonatus* off Namibia. Marine Micropaleontology 66, 120-133.

Sarnthein, M., Winn, K., Jung, S.A., Duplessy, J.C., Labeyrie, L., Erlenkeusser, H., Ganssen, G., 1994. Changes in east Atlantic deepwater circulation over the last 30,000 years: Eight time slice reconstructions. Paleoceanography 9, 209-267.

Sarnthein, M., Stattegger, K., Dreger, D., Erlenkeuser, H., Grootes, P.M., Haupt, B.J., Jung, S.J.A, Kiefer, T., Kuhnt, W., Pflaumann, U., Schäfer-Neth, C., Schulz, H., Schulz, M., Seidov, D., Simstich, J., van Kreveld, S.A., Vogelsang, E., Völker, A.,

Weinelt, M., 2001. Fundamental modes and abrupt changes in North Atlantic circulation and climate over the last 60 ky - concepts, reconstruction and numerical modeling. In: Schäfer, W; Ritzrau, M; Schlüter & J. Thiede (eds.) The Northern North Atlantic: A Changing Environment, Springer Verlag, Berlin, 500 pp.

Schmiedl, G., Pfeilsticker, M., Hemleben, C., Mackensen, A., 2004. Environmental and biological effects on the stable isotope composition of recent deep-sea benthic foraminifera from the western Mediterranean Sea. Marine Micropaleontology 51, 129-152.

Schmiedl, G., Mackensen, A., 2006. Multispecies stable isotopes of benthic foraminifers reveal past changes of organic matter decomposition and deepwater oxygenation in the Arabian Sea. Paleoceanography 21, doi:10.1029/2006PA001284.

Shackleton, N.J., 1974. Attainment of isotopic equilibrium between ocean water and benthonic foraminifera genus Uvigerina: isotopic changes in the ocean during the last glacial. In Labeyrie, L. (ed.): Variation du climat au cours du Pleistoceene, 203–209. Colloques Internationau x du Centre Nationale de la Recherche Scientifique 219.

Shackleton, N.J, Hall, M., Vincent, E., 2000. Phase relationships between millennial-scale events 64,000-24,000 years ago. Paleoceanography 15, 565-569.

Shackleton, N.J., Fairbanks, R.G., Chiu, T.-C., Parrenin, F., 2004. Absolute calibration of the Greenland time scale: implications for Antarctic time scales and for Δ14C. Quaternary Science Reviews 23, 1513-1522.

Spero, H.J., Bijma, J., Lea, D.W., Bemis, B.E., 1997. Effect of seawater carbonate concentration on foraminiferal carbon and oxygen isotopes. Nature 390, 497-500.

Voelker, A.H.L., Sarnthein, M., Grootes, P.M., Erlenkeuser, H., Laj, C., Mazaud, A., Nadeau, M.J.; Schleicher, M., 1998. Correlation of marine 14C-ages from the Nordic Seas with the GISP2 isotope record: Implications for radiocarbon calibration beyond 25ka BP. Radiocarbon 40, 517-534.

Voelker, A., Lebreiro, S.M., Schönfeld, J., Cacho, I, Erlenkeuser, H., Abrantes, F., 2006. Mediterranean outflow strengthening during northern hemisphere coolings: A salt source for the glacial Atlantic? Earth and Planetary Science Letters 245, 39-55.

Vogelsang, E., 1990. Paläo-Ozeanographie des Europäischen Nordmeeres an Hand stabiler Kohlenstoff- und Sauerstoffisotope. Berichte aus dem Sonderforschungsbereich 313, Christian-Albrechts-Universität, Kiel, 23, 136 pp.

Wang, L., Sarnthein, M., Erlenkeuser, H., Grimalt, J.O., Grootes, P.M., Heilig, S., Ivanova, E.V., Kienast, M., Pelejero, C., Pflaumann, U., 1999. East-Asian monsoon climate during the Late Pleistocene: high-resolution sediment records from the South China Sea. Marine Geology 156, 245-284.

Waelbroeck, C., Labeyrie, L., Michel, E., Duplessy, J.C., McManus, J.F., Lambeck, K., Balbon, E., Labracherie, M., 2002. Sea-level and deep water temperature changes derived from benthic foraminifera isotopic records. Quaternary Science Reviews 21, 295-305.

Weinelt, M., 1993. Veränderungen der Oberflächenzirkulation im Europäischen Nordmeer während der letzten 60.000 Jahre - Hinweise aus stabilen Isotopen. Berichte aus dem Sonderforschungsbereich 313, Christian-Albrechts-Universität, Kiel, 41, 106 pp.

Winn, K., Sarnthein, M., Erlenkeuser, H., 1991. $\delta^{18}O$ Stratigraphy and Chronology of Kiel Sediment Cores from the East Atlantic. Berichte-Reports, Geologisch-Paläontologisches Institut und Museum, Christian-Albrechts-Universität, Kiel, 45, 99 pp.

Wollenburg, J.E., Kuhnt, W., Mackensen, A., 2001. Changes in Arctic Ocean paleoproductivity and hydrography during the last 145 kyr: the benthic foraminiferal record. Paleoceanography 16, 65-77.

Woodruff, F., Savin, S.M., Douglas, R.G., 1980. Biological fractionation of oxygen and carbon isotopes by recent benthic foraminifera. Marine Micropaleontology 5, 3-11.

Yu, J., Elderfield, H., Piotrowski, A.M., 2008. Seawater carbonate-ion-δ13C systematics and application to glacial-interglacial North Atlantic ocean circulation. Earth and Planetary Science Letters 271, 209-220.

Zahn, R., Winn, K., Sarnthein, M., 1986. Benthic foraminiferal $\delta^{13}C$ and accumulation rates of organic carbon: Uvigerina peregrina group and Cibicidoides wuellerstorfi. Paleoceanography 1, 27-42.

Zahn-Knoll, R., 1986. Spätquartäre Entwicklung von Küstenauftrieb und Tiefenwasserzirkulation im Nordost-Atlantik. Rekonstruktion anhand stabiler Isotope kalkschaliger Foraminiferen. Diploma Thesis, Geologisch-Paläontologisches Institut, Christian-Albrechts-Universität, Kiel, 111 pp.

Zeebe, R., 1999. An explanation of the effect of seawater carbonate concentration on foraminiferal oxygen isotopes. Geochimica et Cosmochimica Acta 63, 2001–2007.

Zhou, G.T., Zheng, Y.F., 2003. An experimental study of oxygen isotope fractionation between inorganically precipitated aragonite and water at low temperatures. Geochimica et Cosmochemica Acta 67, 387-399.

Figure 1. Location details of benthic foraminiferal isotope records used in this study, with 1) PS2212-3, 2) PS1730-2, 3) V27-60, 4) PS1243-1, 5) GIK23065-3, 6) PS2644-5, 7) V27-86, 8) SU90-39, 9) SU90-11, 10) CH72-02, 11) MD95-2042, 12) MD99-2339, 13) GIK11944-2, 14) CH74-227, 15) GIK15666-6, 16) KNR140-2 JPC-37, 17) GIK16006-1, 18) GIK15637-1, 19) GIK12309-2, 20) GIK12392-1, 21) GIK12379-1, 22) GIK16030-1, 23) GIK12328-5, 24) GIK13289-2, 25) GIK12347-2, 26) GIK16402-2, 27) GIK13239-1, 28) GIK13519-1, 29) GIK16856-2, 30) INMD-115BX, 31) V29-135, 32) TTN057-6, 33) TR126-29, 34) TR126-23, 35) MD84-560, 36) MD88-770, 37) MD77-194, 38) GeoB3004-1, 39) GIK17940-2 (Bauch et al., 2001; Berger et al., 1985; Bühring, 2001; Climap project members, 1981; Curry et al., 1988; Duplessy, 1996; Duplessy et al., 1988; Hagen and Keigwin, 2002; Hodell et al., 2003; Labeyrie and Duplessy, 1985; Labeyrie et al., 1995; 1996; Sarnthein et al., 2001; Voelker et al., 1998; 2006; Vogelsang, 1990; Wang et al., 1999; Weinelt, 1993; Winn et al., 1991; Wollenburg et al., 2001; Zahn-Knoll, 1986; Zahn et al., 1986). Map was made using the online map creation website http://www.aquarius.geomar.de.

Figure 2. A- Histograms showing benthic foraminiferal $\delta^{18}O$ offsets for *C. wuellerstorfi* vs. *U. peregrina* (CW-UP), *U. hollicki* (CW-UH), *M. barleeanum* (CW-MB), *G. affinis* (CW-GA) and *U. peregrina* vs. *G. affinis* (UP-GA). B- Cross plots of the same benthic foraminiferal pairs. Holocene (0-10 ka) samples are indicated with small orange circles, MIS 5e samples with large red circles, glacial samples with small blue circles (full glacial sample 18-21 indicate with big dark blue circles). Normal linear interpolations through the data are shown in black lines, whereas linear interpolations forced through the origin are shown in black stippled lines. Cross plots and histograms for remaining benthic foraminiferal pairs with less data points (< 100) or from only 1 down-core record can be found in online supporting material Figure S1. For the correlations either a normal linear correlation or a linear correlation through 0, 0 produce similar correlation coefficients (R) for the datasets. However in sets where the correlation is weaker, a linear correlation through 0, 0 gives a much lower R (Figure S1).

Figure 3. Examples of individual benthic foraminiferal $\delta^{18}O$ (top; epifaunal in black, infaunal in grey) records and offset records (bottom). Where available locations of

AMS ^{14}C ages or calendar ages are projected as grey diamonds or grey boxes. Major isotope stages (after SPECMAP) are indicated at the top. Black straight lines represent the mean record $\delta^{18}O$ offsets, with grey background boxes delineating the standard deviation. Offsets are plotted against depth (m) rather than age to minimise the role of interpretation with regards to age models, and to emphasize extent of depths with varying isotope offsets involved. Benthic foraminiferal oxygen isotope offset records are divided into three categories: A- records showing no temporal variations in benthic foraminiferal $\delta^{18}O$ offset, B- records showing small (0.2-0.5‰) temporal variations in benthic foraminiferal $\delta^{18}O$ offset, and C- records showing large (>0.5‰) temporal variations in benthic foraminiferal $\delta^{18}O$ offset. All other records can be found in online supporting material Figure S2. Data are from Sarnthein et al. (1994), Shackleton et al. (2000) and Schmiedl and Mackensen (2006). AMS ages MD95-2042 (19600 to 46400 ^{14}C years with 500 year reservoir correction) are from Shackleton et al. (2004). Also indicated are averaged interglacial (Holocene 0-10 ka; MIS 5e 115-126 ka) benthic foraminiferal offsets in red and full glacial (18-21 ka) benthic foraminiferal offsets in blue. Only cores where differences in offset exceed that of the standard deviation of the offset were classified as having temporal variations.

Figure 4. Epifaunal and infaunal benthic foraminiferal $\delta^{13}C$ (top) and gradients (bottom) plotted with benthic foraminiferal $\delta^{18}O$ offset records (bottom; grey) for same cores as Figure 3, with: A- records showing no temporal variations in benthic foraminiferal $\delta^{18}O$ offset, B- records showing small (0.2-0.5‰) temporal variations in benthic foraminiferal $\delta^{18}O$ offset, and C- records showing large (>0.5‰) temporal variations in benthic foraminiferal $\delta^{18}O$ offset. All other records can be found in online supporting material Figure S3. Data are from Sarnthein et al. (1994), Shackleton et al. (2000) and Schmiedl and Mackensen (2006).

Figure 5. Overview of cores (and water depths) with >15 sample pairs and well constrained age models, showing temporal (black & grey circles) or no temporal (white circles) variability in benthic foraminiferal $\delta^{18}O$ offset for the last <150,000 years. Black and grey circles with a white stripe across represent cores where temporal variations in the $\delta^{18}O$ offset between *C. wuellerstorfi* and *U. peregrina* and/or *U. hollicki* were detected. At GIK 12309 (19), GIK 16030 (22), and GIK

12328-5 (23) (grey circles white stripe across), the glacial-interglacial offset variations are caused by depleted glacial *U. peregrina* $\delta^{18}O$, whereas at KNR140-37JPC(16), GIK 12392-1(20), GIK 13239-1(27), GIK 13519 (28), V29-135 (31), and GeoB3004-1 (38), (black circles white stripe across), the partly more negative interglacial offsets are caused by the *Uvigerina* species not showing the (full) deglacial/interglacial decrease in $\delta^{18}O$.

Figure 6. Histograms of benthic foraminiferal $\delta^{18}O$ offsets of original and edited *C. wuellerstorfi* vs. *U. peregrina* and *U. peregrina* vs. *G. affinis* (A, A') and cross plots (B, B'). Exclusion of deglacial/interglacial enriched *U. peregrina* and *G. affinis* samples, and glacial depleted *U. peregrina* samples (in both cases where the difference in offset exceeded the standard deviation of the offset) reduces the standard deviation of the mean $\delta^{18}O$ offset and improves the linear correlations (A', B').

Species	Mean $\delta^{18}O$ offset ± S.D. (number of cores, sample pairs) in ‰.	Individual records (sample pairs ≥ 20)	$\delta^{18}O$ offset ± S.D. per core in ‰.	Holocene MIS 5e (‰)	Full glacial (‰)	ΔIG-G > S.D
C. wuellerstorfi- P. arimensis	0.43 ± 0.44 (2, 60)					
		15, GIK15666-6 (33)	0.39 ± 0.45	0.88 (5)	0.24 (3)	YES
		17, GIK16006-1 (27)	0.49 ± 0.42	0.43 (2)	-0.04 (1)	YES
C. lobatulus- C. pachyderma	0.07 ± 0.56 (2, 41)					
		12, MD99-2339 (29)	0.21 ± 0.21			N.C./NO
C. wuellerstorfi- C. kullenbergi	-0.06 ± 0.38 (6, 48)					
		32, TTNO57-6 (29)	-0.03 ± 0.23	-0.21 (1) -0.02 (9)		NO
C. wuellerstorfi- U. peregrina	-0.72 ± 0.35 (12, 645)					
		11, MD95-2042 (69)	-0.72 ± 0.17	-0.83 (2)	-0.71 (7)	NO
		16, KNR140-2 JPC-37 (109)	-0.60 ± 0.23	-1.09 (1)	-0.55 (1)	YES
		19, GIK12309-2 (18)	-0.60 ± 0.28	-0.72 (3)	-0.29 (3)	YES
		20, GIK12392-1 (47)	-0.77 ± 0.43	-0.48 (3) -1.69 (4)		NO (but yes other interval)
		21, GIK12379-1 (29)	-0.72 ± 0.15	-0.71 (11)	-0.72 (3)	NO
		22, GIK16030-1 (25)	-0.10 ± 0.54	-0.63 (5)	+0.60 (3)	YES
		23, GIK12328-5 (67)	-0.71 ± 0.18	-0.73 (16)	-0.42 (6)	YES
		24, GIK 13289-2 (26)	-0.82 ± 0.19	-0.80 (7)	-0.85 (4)	NO
		25, GIK12347-2 (31)	-0.82 ± 0.13	-0.75 (9)	-0.74 (4)	NO
		31, V29-135 (55)	-1.01 ± 0.34	-0.84(2) -1.34 (4)	-0.66 (2)	YES
		38,GeoB3004-1 (149)	-0.74 ± 0.39	-1.58 (8) -1.15 (13)	-0.71 (7)	YES
C. wuellerstorfi- U. hollicki	-0.69 ± 0.27 (6, 236)					
		20, GIK12392-1 (95)	-0.73 ± 0.22	-0.65 (9)	-0.68 (6)	POT

				-0.87 (6)		
		20, GIK12392-1 (34)	-0.66 ± 0.30	-0.59 (5) -1.64 (1)	-0.42 (5)	POT
		27, GIK13239-1 (40)	-0.72 ± 0.25	-1.02 (4)	-0.63 (5)	YES
		28, GIK13519-1 (32)	-0.60 ± 0.26			N.C. (but yes other interval)
C. wuellerstorfi- U. excellens	-0.99 ± 0.66 (4, 89)					
C.wuellerstorfi-U. mediterranea	-0.46 ± 0.65 (1, 22)	**15, GIK15666-6**		0.67 (3)	-0.58 (1)	YES
C. wuellerstorfi- O. umbonatus	-0.52 ± 0.59 (4, 85)					
		4, PS1243-1 (48)	-0.73 ± 0.45	-0.38 (10)	-1.24 (5)	YES
		30, INMD-115BX (20)	-0.50 ± 0.37	-0.40 (8)	-0.32 (2)	NO
C. wuellerstorfi- O. tener	-0.57 ± 0.45 (3, 67)					
		5, GIK23065-3 (36)	-0.34 ± 0.19			N.C./NO
C. wuellerstorfi- M. barleeanum	-0.18 ± 0.24 (4, 162)					
		38, GeoB3004-1 (147)	-0.17 ± 0.25	-0.52* (11) -0.15 (11)	-0.19 (6)	YES
C. wuellerstorfi- G. affinis	-0.90 ± 0.25 (2, 277)					
		11, MD95-2042 (128)	-0.99 ± 0.15			N.C.
		38, GeoB3004-1 (174)	-0.83 ± 0.28	-0.66 (10) -0.70 (9)	-0.75 (6)	NO
U. peregrina - M. barleeanum	0.55 ± 0.37 (1, 142)	38, GeoB3004-1		1.20 (6) 0.97 (10)	0.57 (6)	YES
U. peregrina- G. affinis	-0.09 ± 0.38 (2, 188)					
		11, MD95-2042 (51)	-0.14 ± 0.16			N.C./NO
		38, GeoB3004-1 (137)	-0.07 ± 0.43	0.83 (10) 0.65 (10	-0.03 (5)	YES
M. barleeanum- G. affinis	-0.65 ± 0.22 (1, 132)	**38, GeoB3004-1**		-0.51 (9) -0.55 (5)	-0.57 (6)	NO

Table 1. Mean offsets ± standard deviation for all benthic foraminiferal $\delta^{18}O$ pairs; between brackets details of number of records and sample pairs are given. In the third and fourth column give individual core details and calculated mean $\delta^{18}O$ offset ± standard deviation for individual records containing > 20 sample pairs. In columns five and six mean interglacial Holocene (0-10 ka)/ MIS 5e (115-126 ka) and full glacial (18-21 ka) benthic foraminiferal $\delta^{18}O$ offsets are calculated. * Indicates early Holocene. Number of sample pairs is indicated between brackets. Finally in column 7 records denoted with YES have an interglacial-glacial difference in benthic foraminiferal $\delta^{18}O$ offset exceeding the standard deviation. (N.C. = not calculated because either interglacial or full glacial data missing; POT = potential interglacial-glacial difference exceeding the standard deviation for both GIK 12392-1 records). Records indicated with NO do not have temporal variations in benthic foraminiferal $\delta^{18}O$ offsets.

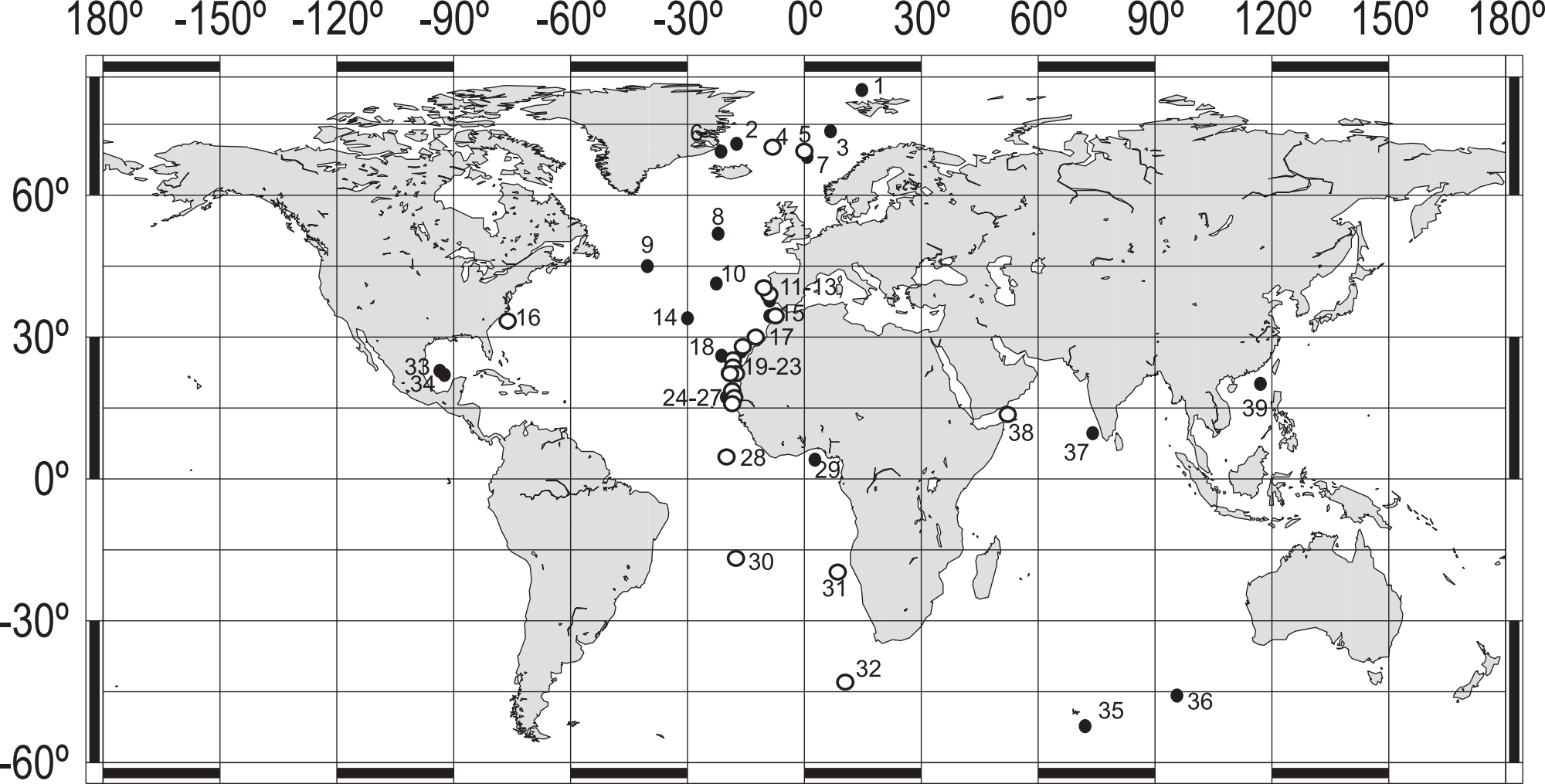
180º -150º -120º -90º -60º -30º 0º 30º 60º 90º 120º 150º 180º
60º
30º
0º
-30º
-60º
1
2
3
4
5
6
7
8
9
10
11-13
14
15
16
17
18
19-23
24-27
28
29
30
31
32
33
34
35
36
37
38
39

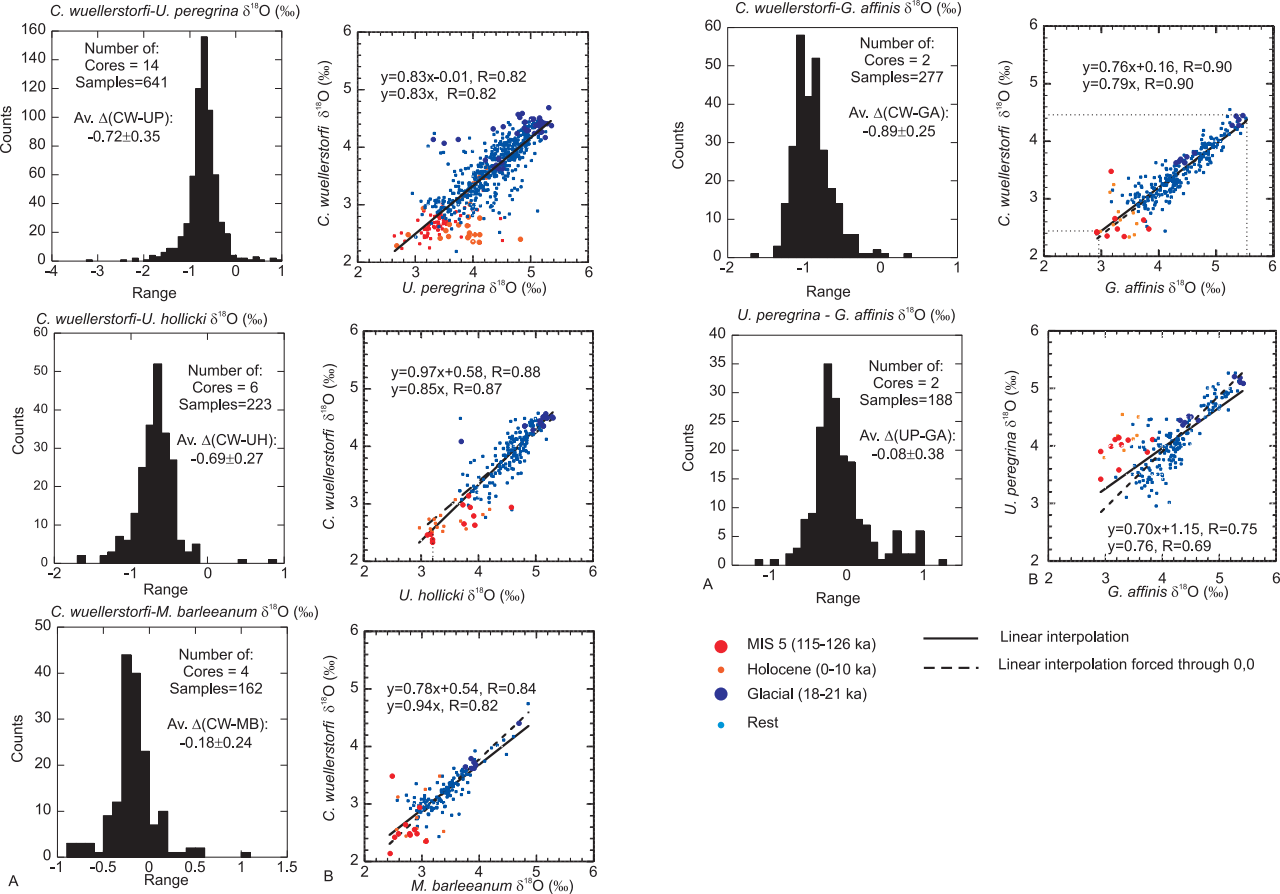
C. wuellerstorfi-U. peregrina δ18O (‰)
Number of:
Cores = 14
Samples=641
Av. Δ(CW-UP):
-0.72±0.35
Counts
Range
y=0.83x-0.01, R=0.82
y=0.83x, R=0.82
C. wuellerstorfi δ18O (‰)
U. peregrina δ18O (‰)
C. wuellerstorfi-G. affinis δ18O (‰)
Number of:
Cores = 2
Samples=277
Av. Δ(CW-GA):
-0.89±0.25
y=0.76x+0.16, R=0.90
y=0.79x, R=0.90
G. affinis δ18O (‰)
C. wuellerstorfi-U. hollicki δ18O (‰)
Number of:
Cores = 6
Samples=223
Av. Δ(CW-UH):
-0.69±0.27
y=0.97x+0.58, R=0.88
y=0.85x, R=0.87
U. hollicki δ18O (‰)
U. peregrina - G. affinis δ18O (‰)
Number of:
Cores = 2
Samples=188
Av. Δ(UP-GA):
-0.08±0.38
y=0.70x+1.15, R=0.75
y=0.76, R=0.69
C. wuellerstorfi-M. barleeanum δ18O (‰)
Number of:
Cores = 4
Samples=162
Av. Δ(CW-MB):
-0.18±0.24
y=0.78x+0.54, R=0.84
y=0.94x, R=0.82
M. barleeanum δ18O (‰)
A
B
MIS 5 (115-126 ka)
Holocene (0-10 ka)
Glacial (18-21 ka)
Rest
Linear interpolation
Linear interpolation forced through 0,0

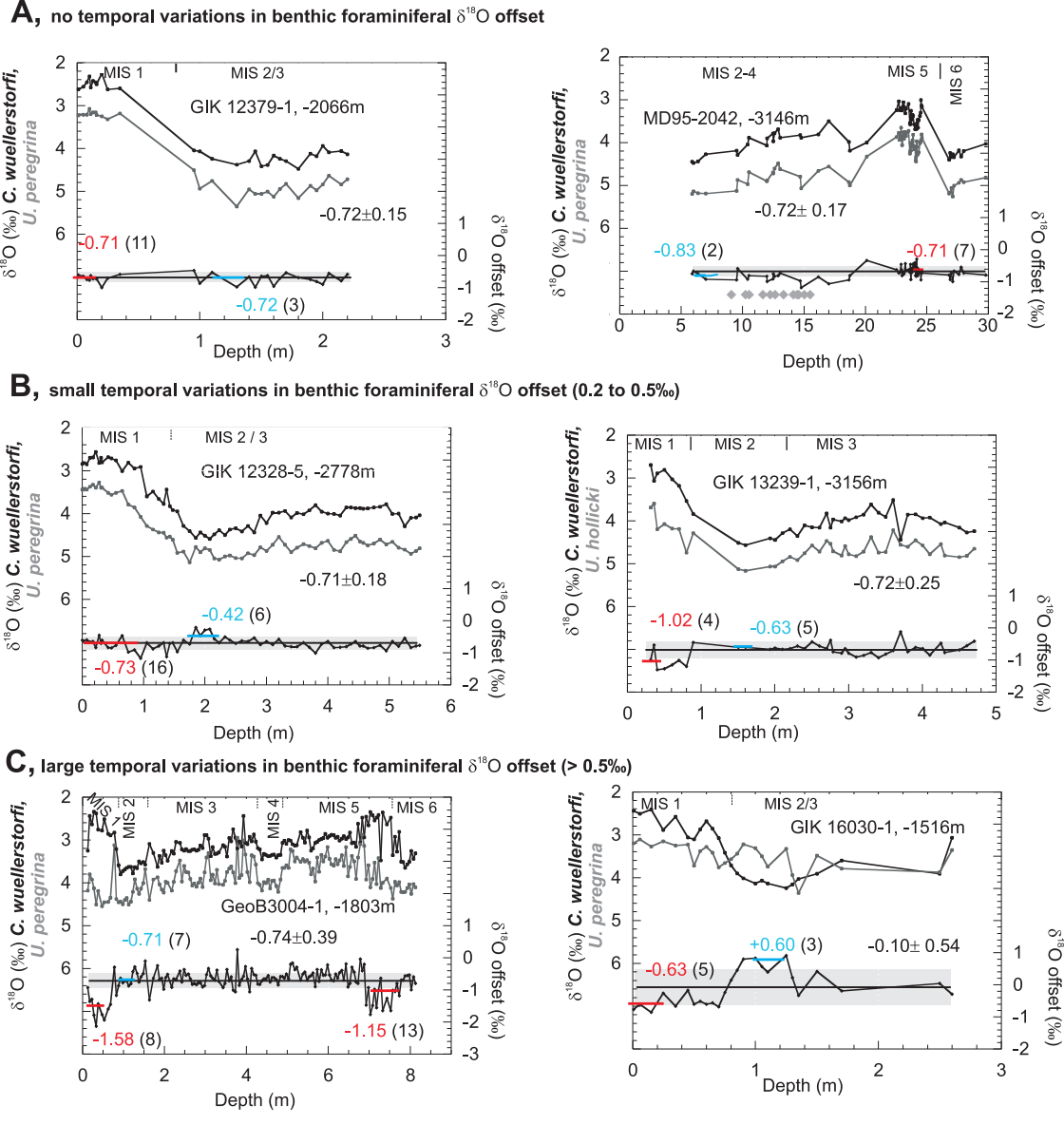
A, no temporal variations in benthic foraminiferal δ18O offset
MIS 1
MIS 2/3
GIK 12379-1, -2066m
-0.72±0.15
-0.71 (11)
-0.72 (3)
δ18O (‰) C. wuellerstorfi, U. peregrina
δ18O offset (‰)
Depth (m)
MIS 2-4
MIS 5
MIS 6
MD95-2042, -3146m
-0.72± 0.17
-0.83 (2)
-0.71 (7)
B, small temporal variations in benthic foraminiferal δ18O offset (0.2 to 0.5‰)
MIS 1
MIS 2 / 3
GIK 12328-5, -2778m
-0.71±0.18
-0.42 (6)
-0.73 (16)
MIS 2
MIS 3
GIK 13239-1, -3156m
δ18O (‰) C. wuellerstorfi, U. hollicki
-0.72±0.25
-1.02 (4)
-0.63 (5)
C, large temporal variations in benthic foraminiferal δ18O offset (> 0.5‰)
MIS 4
MIS 5
MIS 6
GeoB3004-1, -1803m
-0.74±0.39
-0.71 (7)
-1.58 (8)
-1.15 (13)
GIK 16030-1, -1516m
-0.10± 0.54
+0.60 (3)
-0.63 (5)

A, no temporal variations in benthic foraminiferal $\delta^{18}O$

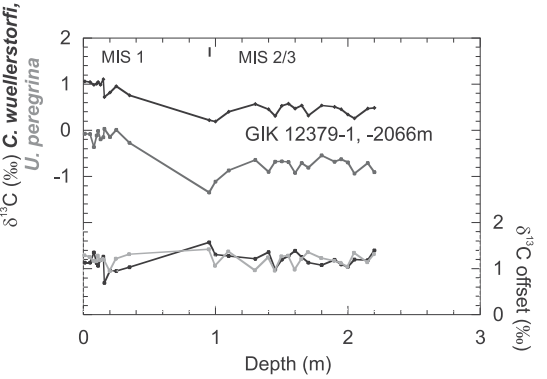

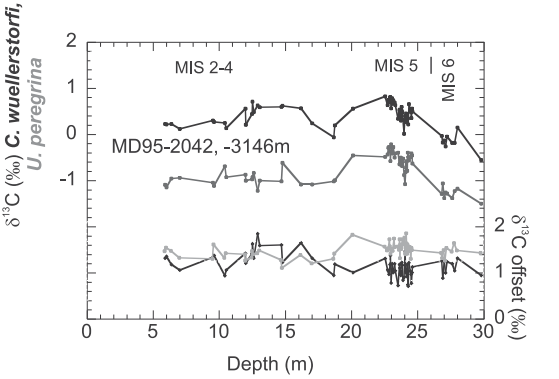

B, small temporal variations in benthic foraminiferal $\delta^{18}O$ (0.2 to 0.5‰)

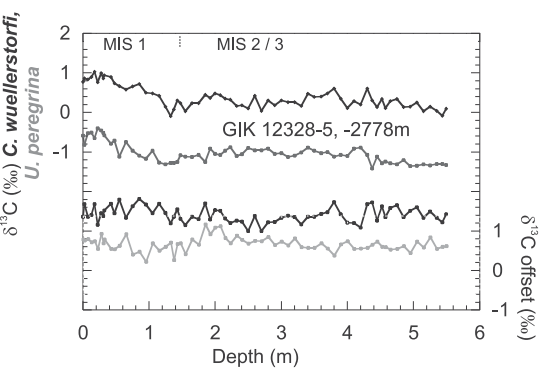

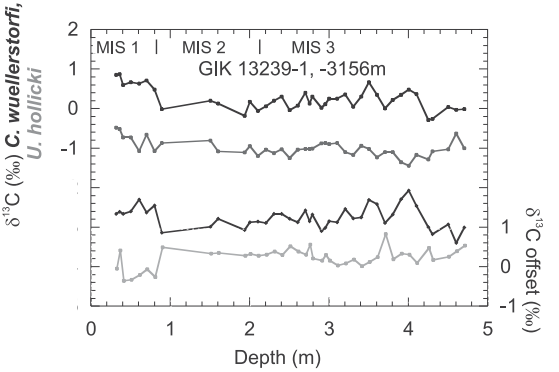

C, large temporal variations in benthic foraminiferal $\delta^{18}O$ (>0.5‰)

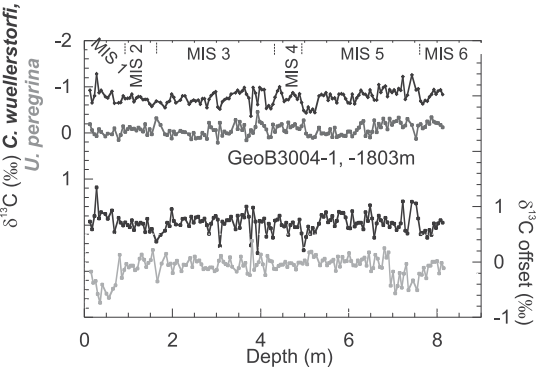

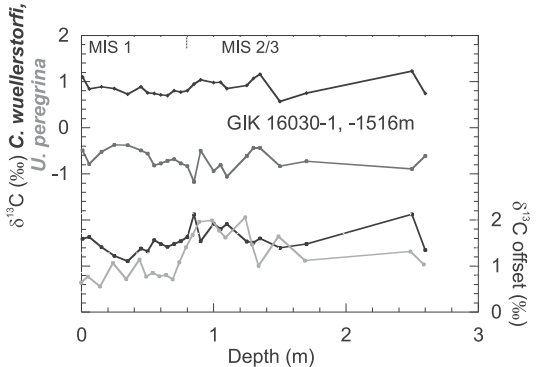

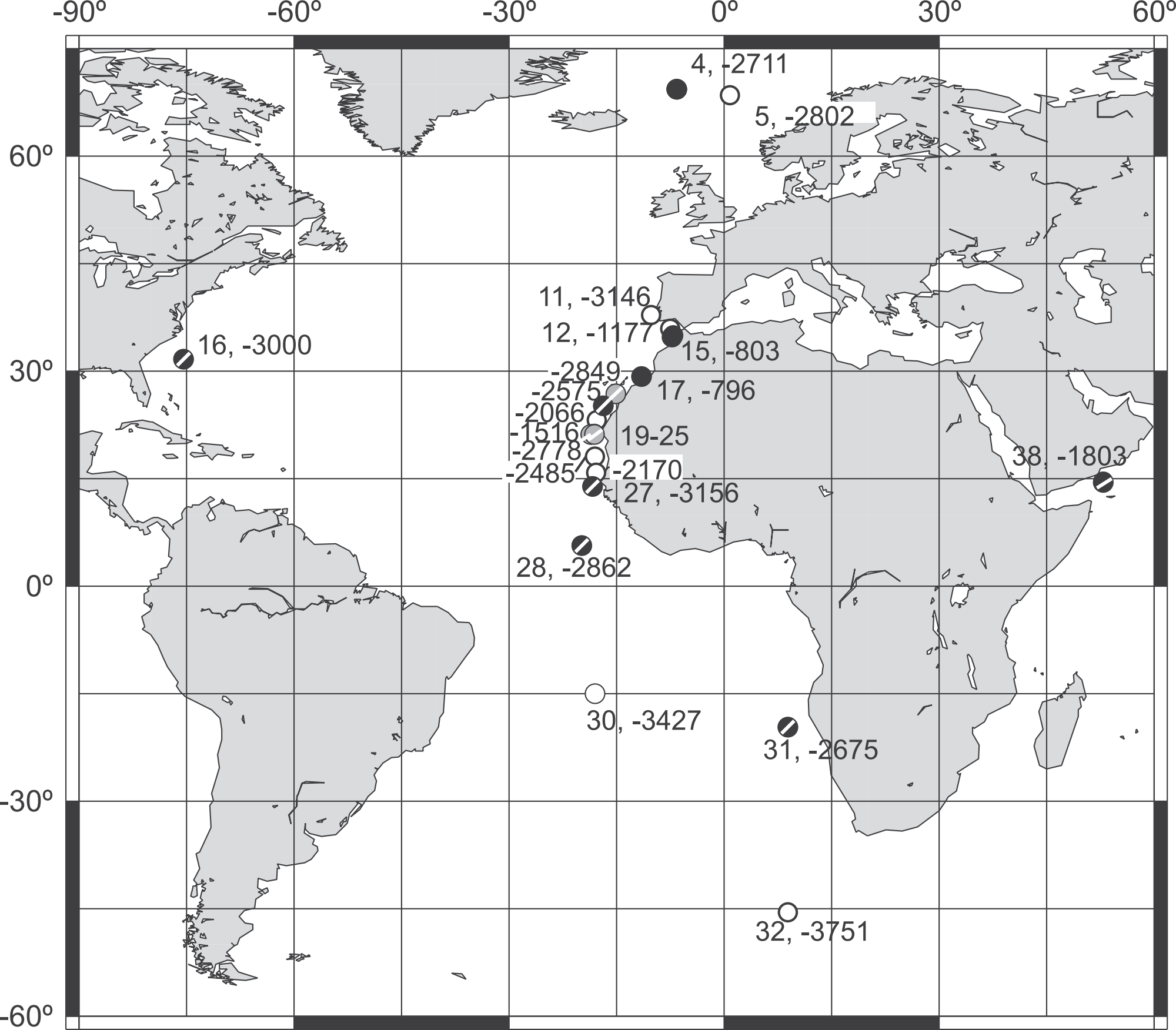
-90°
-60°
-30°
0°
30°
60°
60°
30°
0°
-30°
-60°
4, -2711
5, -2802
11, -3146
12, -1177
15, -803
16, -3000
-2849
17, -796
-2575
-2066
-1516
19-25
-2778
-2485
-2170
27, -3156
38, -1803
28, -2862
30, -3427
31, -2675
32, -3751

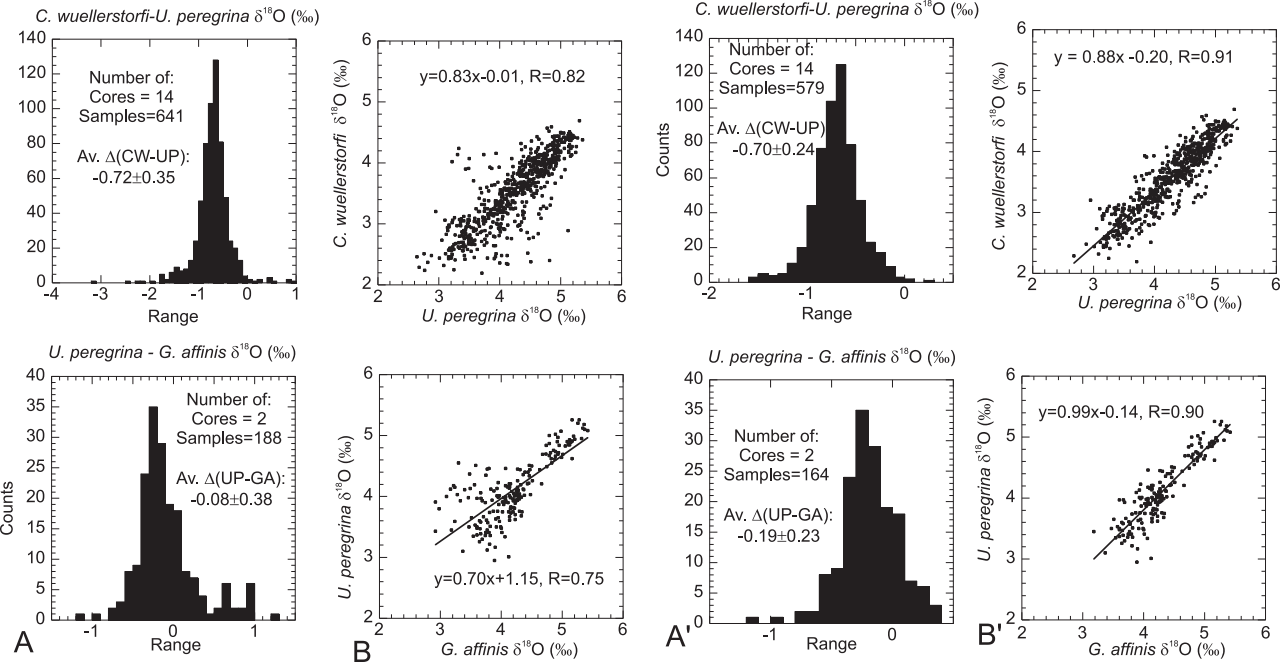
C. wuellerstorfi-U. peregrina δ18O (‰)
Number of:
Cores = 14
Samples=641
Av. Δ(CW-UP):
-0.72±0.35
Range
y=0.83x-0.01, R=0.82
C. wuellerstorfi δ18O (‰)
U. peregrina δ18O (‰)
C. wuellerstorfi-U. peregrina δ18O (‰)
Number of:
Cores = 14
Samples=579
Av. Δ(CW-UP)
-0.70±0.24
Counts
Range
y = 0.88x -0.20, R=0.91
C. wuellerstorfi δ18O (‰)
U. peregrina δ18O (‰)
U. peregrina - G. affinis δ18O (‰)
Number of:
Cores = 2
Samples=188
Av. Δ(UP-GA):
-0.08±0.38
Counts
Range
A
y=0.70x+1.15, R=0.75
U. peregrina δ18O (‰)
G. affinis δ18O (‰)
B
U. peregrina - G. affinis δ18O (‰)
Number of:
Cores = 2
Samples=164
Av. Δ(UP-GA):
-0.19±0.23
Range
A'
y=0.99x-0.14, R=0.90
U. peregrina δ18O (‰)
G. affinis δ18O (‰)
B'